Reducing the critical current for short-pulse spin-transfer switching of nanomagnets

P. M. Braganca,[a] I. N. Krivorotov, O. Ozatay, A. G. F. Garcia, N. C. Emley, J. C. Sankey, D. C. Ralph, and R. A. Buhrman
Cornell University, Ithaca, New York 14853-2501

(Received 22 April 2005; accepted 25 July 2005; published online 9 September 2005)

We have fabricated permalloy/copper/permalloy nanopillar spin valves designed to reduce the critical current for spin-transfer switching while maintaining thermal stability of the free layer. Pulsed current amplitudes necessary for switching a 4.5-nm-thick permalloy free layer range from 0.4 mA for a 100 ns pulse to 2 mA for a 1 ns pulse, showing that the magnetization must be overdriven to achieve switching on short time scales. Comparisons to Landau–Lifshitz–Gilbert simulations indicate an effective damping parameter ≈ 0.03 and spin-torque efficiencies for parallel-to-antiparallel and antiparallel-to-parallel switching that are more symmetric than predicted by recent theoretical models. © *2005 American Institute of Physics*. [DOI: 10.1063/1.2045552]

Following the prediction[1,2] and demonstration[3,4] of the spin-transfer switching effect, the use of a spin-polarized current to reversibly switch the orientation of a thin-film nanomagnet has been considered for future high-speed, nonvolatile nanoscale magnetic memory systems.[5] Several advances are needed to move this possibility closer to practical reality, with one being a reduction in the currents (I_c) and the current densities (J_c) required to exert sufficient spin torque for 1–10-ns-scale switching. Recent studies[6,7] have demonstrated that spin-transfer switching can occur on time scales as short as 100 ps, but this requires currents on the order of 10 mA. In contrast, switching currents on the order of 0.1–0.2 mA are required for making high-density memory circuits using minimum-area metal–oxide–semiconductor field-effect transistors. Strategies for reducing I_c must be subject to the added constraint that the nanomagnet remains thermally stable, which means that devices must use nanomagnets with an energy barrier to reversal $U_A(T) \geqslant 1.0$ eV when operating at room temperature (RT), or an even larger barrier (>1.3 eV) for an operating temperature of 100 °C. One approach is to employ nanomagnets with large shape anisotropy and low saturation magnetization. While further improvements are still needed, here we report results from stable spin-valve nanopillar devices that can be switched on the nanosecond time scale with pulse current amplitudes <1 mA.

Calculations of spin-transfer switching predict that I_c for a thin-film nanomagnet should scale as $I_c \sim M_s^2 V\alpha$, where M_s is the nanomagnet's saturation magnetization, V its volume, and α the Gilbert damping parameter.[3,8] This holds if the nanomagnet's demagnetization field $4\pi M_s \gg 2(H_k + H_{\text{applied}})$, as is the usual case for such thin-film nanomagnets, where H_k is the in-plane shape anisotropy field. In contrast, $U_A \sim H_k M_s V$, so minimizing I_c without reducing U_A requires maximizing H_k while decreasing M_s. Since H_k increases with film thickness, one should be able to produce a thermally stable nanomagnet with a low I_c by fabricating a comparatively thick nanomagnet structure with pronounced shape anisotropy from a material with small average M_s.

We have used electron-beam lithography to pattern magnetic nanopillar structures with high-aspect-ratio (3:1) elliptical cross sections, employing proximity effect corrections to obtain the desired shape in the exposed pattern. These patterns were ion-beam etched into sputtered multilayer stacks of (all dimensions in nm) 120 Cu/20 Py/12 Cu/X Py/2 Cu/30 Au, where Py is permalloy ($Ni_{81}Fe_{19}$) and the thickness X of the Py free layer is either 4.5 or 7 nm. The devices were contacted as described previously.[9] Figure 1(a) shows a scanning electron microscope image of an approximately elliptical nanopillar having a 40 nm minor axis and a 3:1 aspect ratio, taken before deposition of the top electrode. Figure 1(b) is a cross-sectional schematic of the device.

Using a 2 nm cubic cell size chosen for simulation convenience, a three-dimensional (3D) micromagnetic simulation (3D OOMMF)[10] of a 4-nm-thick film of Py with a perfectly elliptical 40 nm × 120 nm cross section predicts $H_k \approx 1100$ Oe, but this neglects the dipole field from our device's fixed layer. Including this effect, we obtain $H_k \approx 900$ Oe, and further simulation of a complete nanopillar structure having the nonideal shape shown in Fig. 1(a) yields $H_k = 785$ Oe for the free layer. In comparison, 4.2 K measurements of the free-layer easy-axis coercive fields for devices with similar structure to the one in Fig. 1(a) yield an average $H_c \approx 500$ Oe. We attribute the difference between

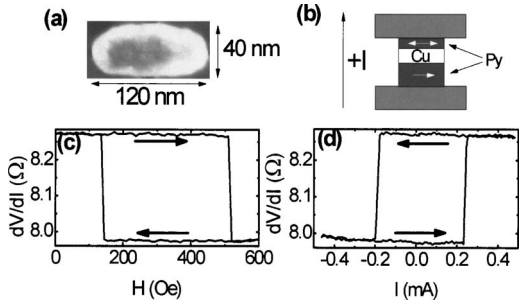

FIG. 1. (a) SEM image of a nanopillar. Patterning with electron-beam lithography produces reproducible approximate ellipses with 40 × 120 nm dimensions. (b) Cross-sectional schematic for nanopillar structure with convention for current direction. (c) Minor loop of free layer and (d) spin transfer curve at 293 K, with convention for current shown in (b) for a typical device.

[a]Electronic mail: pmb32@cornell.edu

the measured H_c and the simulated H_k to the difference between the 4.2 K saturated magnetization of the simulated ideal Py material (M_s=880 emu/cm^3) and that determined by superconducting quantum interference device magnetometry of a thin Py layer sandwiched between Cu films (M_s =645 emu/cm^3), as well as to thin-film roughness which was not modeled in the OOMMF simulation. Using the measured 4.2 K values we obtain $U_A(4.2\ \mathrm{K})=M_sH_kV/2\approx 1.7$ eV.

A typical magnetoresistance field scan of the free layer taken with the fixed-layer magnetization orientation held fixed (minor loop) is shown in Fig. 1(c), and in Fig. 1(d) we show a spin-transfer scan for the same device. The minor loop was taken at T=293 K for applied magnetic field excursions about the value that cancels out the average dipole field from the fixed layer and shows transitions that are thermally activated due to the finite value of $U_A(T)/k_BT$. Here $U_A(T)$ is smaller than $U_A(0)$ due to both the T dependence of M_s and H_k, and more importantly, nonideal or nonmacrospin pathways for thermally activated reversal. The latter is generally modeled[11] by assuming a fictitious applied field H_e such that $U_A(T)=[M_s(T)H_k(T)V/2](1-H_e/H_k)^2$. Typically $H_e/H_k\leqslant 0.5$ for thin-film nanomagnets.[11,12]

To determine U_A (293 K), we made measurements of the average spin-transfer switching current, $\langle I_c\rangle$, from twenty individual scans. This process was then repeated for several different current sweep rates. The results were analyzed with a Kurkijarvi-type treatment of Neel-Brown thermally-activated magnetic reversal due to a spin torque.[5,12–14] In this model we have

$$\langle I_c\rangle = I_{c0}\left[1-\frac{k_BT}{U_A}\ln\left[\frac{1}{\tau_0}\frac{k_BT}{U_A}\frac{|I_{c0}|}{|\dot{I}|}\right]\right], \tag{1}$$

where I_{c0} is the zero temperature critical current, and $\dot{I}$ is the current sweep rate. In Fig. 2(a), we plot $\langle I_c\rangle$ for a 4.5-nm-thick free layer as a function of $\dot{I}$ for transitions in which the free-layer moment is driven from parallel to the fixed-layer moment to antiparallel (P–AP) and vice versa (AP–P). Assuming a fluctuation attempt time τ_0=1 ns,[12] we obtain $U_{A,\text{P-AP}}(293\ \mathrm{K})=0.85\pm0.03$ eV, $I_{c0,\text{P-AP}}=0.42\pm0.03$ mA and $U_{A,\text{AP-P}}(293\ \mathrm{K})=0.73\pm0.01$ eV, $I_{c0,\text{AP-P}}=0.39\pm0.02$ mA. The difference in the two activation energies is qualitatively consistent with OOMMF simulations, which show that the dipole field from the fixed layer has a stronger perturbative effect on the free layer when it is in the AP state than when in the P state. Using the measured 293 K value of M_s (560 emu/cm^3), we would expect $U_{A0}(293\ \mathrm{K})=1.3$ eV, so the fitted values correspond to $H_e/H_k\approx 0.25$. Similar measurements for a 7-nm-thick free-layer sample yielded $U_{A,\text{P-AP}}(293\ \mathrm{K})=2.12\pm0.1$ eV, $I_{c0,\text{P-AP}}=0.77\pm0.01$ mA, and $U_{A,\text{AP-P}}(293\ \mathrm{K})=1.92\pm0.24$ eV, $I_{c0,\text{AP-P}}=0.50\pm0.02$ mA, showing activation energies close to what would be expected from the difference in thickness between 4.5 and 7 nm.

While I_{c0} is the minimum current for spin-torque switching in the absence of significant thermal activation, fast switching requires higher currents. In the short-pulse regime, the switching time varies approximately as $\tau\sim 1/(I-I_{c0})$, with thermal effects resulting in a statistical distribution about this mean value.[8,11] We have measured the switching probability of our nanopillar devices as a function of pulse amplitude I, for pulse widths ranging from 100 to 1 ns. In Fig. 2, we show results of both positive (P–AP) and negative (AP–P) current-pulse switching for a 4.5 nm device. $I>4-5\ I_{c0}$ is required to obtain a high probability of switching with 1 ns pulses.

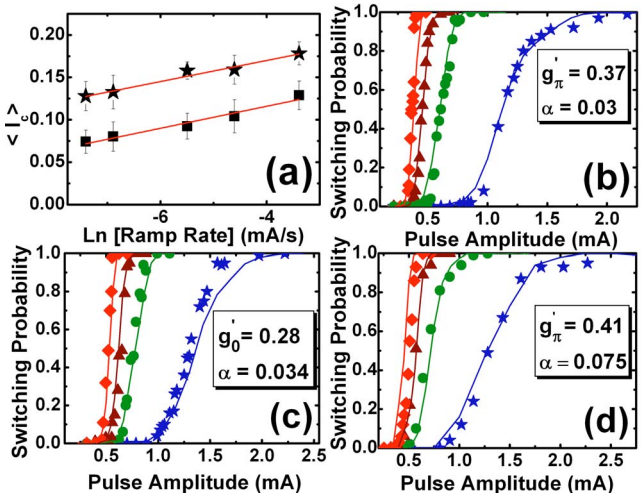

FIG. 2. (Color online) (a) Average switching current vs natural log of current ramp rate for a 4.5 nm Py free layer in the P–AP (★) and AP–P (■) switching directions. Error bars represent dispersion in switching current for 20 current sweeps at a given ramp rate. Lines shown are fits to data with a Kurkijarvi-type model. Switching probabilities vs pulse amplitude and single-domain simulation fits for (b) AP–P and (c) P–AP transitions of a 4.5 nm Py free layer. Pulse widths for each curve from left to right are 100 ns (♦), 10 ns (▲), 3 ns (●), and 1 ns (★). Lines drawn are curves through points generated by LLG simulation. (d) Switching probabilities vs pulse amplitude and simulations (solid lines) for AP–P switching of a 0.6 nm CoFe/5.5 nm PyCu free layer. All measurements were taken at 293 K.

We use the Landau–Lifshitz–Gilbert (LLG) equation macrospin model of the nanomagnet, as modified to include the spin-torque effect,[1,11] to simulate the distribution of short-pulse switching probabilities. This equation can be written as:

$$\frac{d\hat{M}}{dt}=\gamma\hat{M}\times(\vec{H}_{\text{eff}}+\vec{H}_{\text{lang}})-\gamma\alpha\hat{M}\times[\hat{M}\times(\vec{H}_{\text{eff}}+\vec{H}_{\text{lang}})]$$
$$-\frac{I\gamma\hbar g(\theta)}{eM_sV\sin(\theta)}(\hat{M}\times\hat{M}_{\text{fixed}}\times\hat{M}), \tag{2}$$

where $\hat{M}$ and $\hat{M}_{\text{fixed}}$ are unit vectors in the direction of the free- and fixed-layer magnetizations, respectively, γ is the gyromagnetic ratio, I is electric current, e is electric charge, α is the Gilbert damping parameter, and H_{eff} is the sum of contributions from the anisotropy, applied, and demagnetization fields. H_{lang} is a random Langevin field simulating temperature effects, with components determined using a Gaussian with zero mean and a standard deviation fixed by α and T.[11,15] The function $g(\theta)$ characterizes the strength of the spin torque exerted on the free-layer nanomagnet as a function of the angle θ between its moment and that of the fixed layer. We assume that $g(\theta)=A\sin(\theta)/[1+B\cos(\theta)]$, where A and B are constants. The strength of the switching torque is determined by the slopes $|dg(\theta)/d\theta|=g_0'$ or g_π' at the mean starting angles (0 for P–AP, π for AP–P), where $g_0'=A/(1+B)$ and $g_\pi'=A/(1-B)$. In simulating the data, we use the activation energies for magnetic reversal obtained from the slow ramp rate measurements to determine the thermal distribution of the angle θ_0 at the initiation of the pulse. We then

vary g_0', g_π', and the Gilbert damping parameter α to obtain fits to the data. Results of the best-fit simulations are also shown in Fig. 2. All three parameters affect the magnitude of current necessary for switching, but α has different consequences than g_0' and g_π' on how the switching probabilities depend on the pulse width, since the influence of H_{lang}, which depends on α, changes between smaller ($\sim$1 ns) and larger ($\sim$100 ns) time scales. Thus, there is a unique combination of g_0', g_π', and α that gives the best agreement with the entire set of measured probability distributions from 1 to 100 ns.

From our fits, we generally find that $g_0' \sim 0.2-0.3$ and $g_\pi' \approx (1-1.3)g_0'$. Several theoretical predictions for $g(\theta)$ have been proposed recently based on different treatments of the effects of nonequilibrium spin populations in the electrodes.[16–18] Our finding that $g_0' \approx g_\pi'$ is in conflict with the prediction that $g_0' \ll g_\pi'$ within some of these models.[16,18] Perhaps this is due to Py having a short spin-relaxation length,[19] comparable to our free-layer thickness, which should act to reduce nonequilibrium electrode effects. The similar values of g_0' and g_π' reflects that the magnitudes of measured critical currents are surprisingly similar for P–AP and AP–P switching, which is advantageous for practical memory devices. Our fits also yield values for the phenomenological damping parameter, $\alpha \sim 0.025-0.035$, which are comparable to recent reports,[20] but are $\sim 4\times$ the damping in bulk Py. This high value could be due to nonequilibrium "spin pumping" effects[21,22] and/or spin relaxation arising from defects generated in the nanopillar fabrication process.

We have also fabricated nanopillar devices with a CoFe(0.6 nm)/$Py_{65}Cu_{35}$(5.5 nm) free layer. For this composite material, $\langle M_s \rangle = 360$ emu/cm^3 at 293 K, and a larger area ellipse (60 nm $\times$ 180 nm) was required for thermal stability. Pulse-switching results for one such device are shown in Fig. 2(d) along with model fits. The torque parameters for this device, $g_0' = g_\pi' = 0.41$, are somewhat larger than is typical for the pure Py devices, presumably due to use of the CoFe cladding layer. However, the damping is also much larger, $\alpha \approx 0.075$. This reduces the advantage of the smaller M_s, so that significantly smaller values of I_c are not achieved.

In summary, we have fabricated high-aspect-ratio, thermally stable nanopillar spin valves that require comparatively low currents for the short-pulse spin-torque switching of the Py and PyCu free layers. Current amplitudes of approximately 4–5 I_{c0}, where I_{c0} is the $T=0$ critical current determined by slow-ramp-rate measurements, are required to ensure switching with 1 ns pulses. Fits to the pulse data using the LLG model indicate a high damping parameter $\alpha \sim 0.025-0.035$, and that the spin-torque function $g(\theta)$ is more symmetric than expected theoretically, with initial slopes $g_0' \approx g_\pi' \sim 0.2-0.3$. Devices with PyCu–alloy free layers have an even higher $\alpha \approx 0.075$. Achieving still lower I_{c0} will require further reductions in the free layer's magnetic moment, coupled with increases in H_k, increases in g_0' and g_π', and/or decreases in α. Additional methods of increasing switching speed for a fixed-pulsed current amplitude include introducing a nonzero equilibrium angle between the free and fixed layers,[14,20] or fabricating devices with two fixed layers, one on either side of the free layer.[23,24] An enhancement in H_k would result from eliminating the dipole field on the free layer through the use of a properly designed synthetic antiferromagnetic fixed layer.

This research was supported by the National Science Foundation (NSF) through its Nanoscale Science and Engineering Center (NSEC) support of the Center for Nanoscale Systems and by the Army Research Office (ARO). Additional support provided by NSF through use of the National Nanofabrication Infrastructure Network/Cornell Nanoscale Facility (NNIN/CNF) facilities and the facilities of the Cornell Materials Research Science and Engineering Center (MRSEC).

[1] J. C. Slonczewski, J. Magn. Magn. Mater. **159**, L1 (1996).
[2] L. Berger, Phys. Rev. B **54**, 9353 (1996).
[3] J. A. Katine, F. J. Albert, R. A. Buhrman, E. B. Myers, and D. C. Ralph, Phys. Rev. Lett. **84**, 3149 (2000).
[4] E. B. Myers, D. C. Ralph, J. A. Katine, R. N. Louie, and R. A. Buhrman, Science **285**, 867 (1999).
[5] F. J. Albert, N. C. Emley, E. B. Myers, D. C. Ralph, and R. A. Buhrman, Phys. Rev. Lett. **89**, 226802 (2002).
[6] S. Kaka, M. R. Pufall, W. H. Rippard, T. J. Silva, S. E. Russek, J. A. Katine, and M. Carey, J. Magn. Magn. Mater. **286**, 375 (2005).
[7] T. Devolder, A. Tulapurkar, K. Yagami, P. Crozat, C. Chappert, A. Fukushima, and Y. Suzuki, J. Magn. Magn. Mater. **286**, 77 (2005).
[8] J. Z. Sun, Phys. Rev. B **62**, 570 (2000).
[9] N. C. Emley, F. J. Albert, E. M. Ryan, I. N. Krivorotov, D. C. Ralph, R. A. Buhrman, J. M. Daughton, and A. Jander, Appl. Phys. Lett. **84**, 4257 (2004).
[10] M. J. Donahue and D. G. Porter, *OOMMF User's Guide, Version 1.0, Technical Report No.* NISTIR 6376 (National Institute of Standards and Technology, Gaithersburg, MD, 1999).
[11] R. H. Koch, J. A. Katine, and J. Z. Sun, Phys. Rev. Lett. **92**, 088302 (2004).
[12] I. N. Krivorotov, N. C. Emley, A. G. F. Garcia, J. C. Sankey, S. I. Kiselev, D. C. Ralph, and R. A. Buhrman, Phys. Rev. Lett. **93**, 166603 (2004).
[13] J. Kurkijarvi, Phys. Rev. B **6**, 832 (1972).
[14] E. B. Myers, F. J. Albert, J. C. Sankey, E. Bonet, R. A. Buhrman, and D. C. Ralph, Phys. Rev. Lett. **89**, 196801 (2002).
[15] J. C. Sankey, I. N. Krivorotov, S. I. Kiselev, P. M. Braganca, N. C. Emley, R. A. Buhrman, and D. C. Ralph, cond-mat/0505733.
[16] J. Xiao, A. Zangwill, and M. D. Stiles, Phys. Rev. B **70**, 172405 (2004).
[17] J. Manschot, A. Brataas, and G. E. W. Bauer, Appl. Phys. Lett. **85**, 3250 (2004).
[18] J. C. Slonczewski, J. Magn. Magn. Mater. **247**, 324 (2002).
[19] S. D. Steenwyk, S. Y. Hsu, R. Loloee, J. Bass, and W. P. Pratt, J. Magn. Magn. Mater. **170**, L1 (1997).
[20] I. N. Krivorotov, N. C. Emley, J. C. Sankey, S. I. Kiselev, D. C. Ralph, and R. A. Buhrman, Science **307**, 228 (2005).
[21] Y. Tserkovnyak, A. Brataas, and G. E. W. Bauer, Phys. Rev. B **67**, 140404 (2003).
[22] B. Heinrich, Y. Tserkovnyak, G. Woltersdorf, A. Brataas, R. Urban, and G. E. W. Bauer, Phys. Rev. Lett. **90**, 187601 (2003).
[23] L. Berger, J. Appl. Phys. **93**, 7693 (2003).
[24] G. D. Fuchs, I. N. Krivorotov, P. M. Braganca, N. C. Emley, A. G. F. Garcia, D. C. Ralph, and R. A. Buhrman, Appl. Phys. Lett. **86**, 152509 (2005).